Heat Transfer—Asian Research, **42** (8), 2013

Casson Fluid Flow and Heat Transfer Past a Symmetric Wedge

Swati Mukhopadhyay,[1] Iswar Chandra Mondal,[1] and Ali J. Chamkha[2]
[1]Department of Mathematics, The University of Burdwan, Burdwan-713104, W.B., India
[2]Manufacturing Engineering Department, The Public Authority for Applied Education & Training, Shuweikh, 70654 Kuwait

Boundary-layer forced convection flow of a Casson fluid past a symmetric wedge is investigated. Similarity transformations are used to convert the governing partial differential equations to ordinary ones and the reduced equations are then solved numerically with the help of the shooting method. Comparisons with various previously published works on special cases are performed and the results are found to be in excellent agreement. A representative set of graphical results is obtained and illustrated graphically. The velocity is found to increase with an increasing Falkner–Skan exponent whereas the temperature decreases. With the rise of the Casson fluid parameter, the fluid velocity increases but the temperature is found to decrease in this case. The skin friction decreases with increasing values of the Casson fluid parameter. It is found that the temperature decreases as the Prandtl number increases and thermal boundary layer thickness decreases with increasing values of the Prandtl number. A significant finding of this investigation is that flow separation can be controlled by increasing the value of the Casson fluid parameter. © 2013 Wiley Periodicals, Inc. Heat Trans Asian Res, 42(8): 665–675, 2013; Published online 19 June 2013 in Wiley Online Library (wileyonlinelibrary.com/journal/htj). DOI 10.1002/htj.21065

Key words: symmetric wedge, Casson fluid, forced convection, heat transfer, similarity transformations, numerical solution

1. Introduction

During the last few decades, laminar boundary-layer flow past a semi-infinite wedge is of considerable practical and theoretical interest. Falkner and Skan [1] investigated the steady incompressible laminar boundary-layer flow past a wedge. In this pioneering work, Falkner and Skan [1] used the similarity transformation method to reduce the partial differential equation to a third-order ordinary differential equation which was solved numerically. A detailed study of the same problem was carried out by Hartree [2]. The effect of a transverse magnetic field on a permeable wedge placed symmetrically with respect to the flow direction in a non-Newtonian fluid has been considered by Hady and Hassanien [3]. The problem of wedge flow has been further studied by Lin and Lin [4]. In the presence of a magnetic field, Watanabe and Pop [5] presented numerical results for MHD free

Contract grant sponsor: UGC, New Delhi, India under the Special Assistance Programme DSA Phase-1.

convection flow over a wedge. On the other hand, Kafoussias and Nanousis [6] investigated the MHD laminar boundary-layer flow over a permeable wedge. Both of these papers considered a wedge immersed in a Newtonian fluid. Later, the MHD forced convection flow adjacent to a non-isothermal wedge was analyzed in detail by Yih [7]. Several researchers, viz., Hossain et al. [8], Chamkha et al. [9], Pantokratoras [10], Mukhopadhyay [11], Pal and Mondal [12], and others, reconsidered the wedge flow problem under various thermo-physical conditions. Kandasamy et al. [13] discussed the influence of chemical reaction on flow past a wedge in the presence of suction/injection. Also, Hossain et al. [14] studied the unsteady boundary-layer flow past a wedge. Kim [15] and Kim and Kim [16] have considered the steady boundary-layer flow of a micropolar fluid past a fixed wedge with constant surface temperature and constant surface heat flux, respectively. Later on, Ishak et al. [17] discussed the MHD micropolar fluid flow past a wedge in the presence of uniform heat flux. The boundary layer flow over a static or a moving wedge in a viscous fluid (regular fluid) has been extended under diverse physical aspects by Riley and Weidman [18] and Ishak et al. [19, 20]. With the help of similarity transformation, they obtained the self-similar equation which was solved numerically. Kandasamy et al. [21] reported the combined effects of variable viscosity, thermophoresis, and chemical reaction on mixed convection flow past a porous wedge embedded in a non-Darcy porous medium. Recently, in the case of a nanofluid, Yacob et al. [22] analyzed the static/moving wedge flow problem.

Boundary-layer flows of non-Newtonian fluids have been a topic of investigation for a long time as it has applications in various industries. The governing equations of non-Newtonian fluids are highly non-linear and much more complicated than that of Newtonian fluids. Due to the complexity of these fluids, no single constitutive equation exhibiting all properties of such fluids is available (Mukhopadhyay [23], Mukhopadhyay and Vajravelu [24]). Several models can be found in this regard. Though considerable progress has been made in the understanding of the flow characteristics of a non-Newtonian fluid, more investigation on different non-Newtonian models is still needed. Most of the works on the wedge flow problem in the literature are limited to the non-Newtonian power-law fluids. Simply because these fluids are mathematically the easiest to be treated among most of the non-Newtonian fluids (Patel and Timol [25]). There are other non-Newtonian models as well. Among them is the Casson fluid model. In the literature, the Casson fluid model is sometimes stated to fit rheological data better than general viscoplastic models for many materials (Mustafa et al. [26, 27], Bhattacharyya et al. [28]). It becomes the preferred rheological model for blood and chocolate (Singh [29]). Casson fluid exhibits a yield stress (Nadeem et al. [30], Kandasamy and Pai [31]). If a shear stress less than the yield stress is applied to the fluid, it behaves like a solid whereas if a shear stress greater than the yield stress is applied, it starts to move (Eldabe and Salwa [32], Dash et al. [33]).

To the best of the authors' knowledge, Casson fluid flow past a symmetric wedge has not yet been addressed in the literature. Keeping this fact in mind, an attempt is made to investigate the flow and heat transfer characteristics for a Casson fluid in the case of a symmetric wedge. With the help of similarity transformations, the governing partial differential equations corresponding to the momentum and energy equations are transformed to ordinary ones. Using the shooting method, a numerical solution of the problem is obtained. Comparisons with various previously published works on special cases are performed and the results are found to be in excellent agreement. The effects of different parameters have been studied in detail with the help of their graphical representations.

2. Formulation of the Problem

We consider a steady, two-dimensional, laminar boundary-layer flow of a non-Newtonian Casson fluid past a symmetrical sharp wedge (Fig. 1) and its velocity is given by $u_e(x) = U_\infty(x/L)^m$ for $m \leq 1$ where L is a characteristic length, U_∞ is the main stream velocity, and m is the wedge angle parameter related to the included angle $\pi\beta_1$ by $m = \beta_1/(2 - \beta_1)$. It is worth mentioning that β_1 is a measure of the pressure gradient. If β_1 is positive, the pressure gradient is negative or favorable, and a negative value of β_1 denotes a positive pressure gradient (adverse). For $m < 0$, the solution becomes singular at $x = 0$, while for $m \geq 0$, the solution can be defined for all values of x.

The rheological equation of state for an isotropic and incompressible flow of a Casson fluid is given by (see Nakamura and Sawada [34], Mustafa et al. [27])

$$\tau_{ij} = \begin{cases} 2(\mu_B + p_y/\sqrt{2\pi})e_{ij}, & \pi > \pi_c \\ 2(\mu_B + p_y/\sqrt{2\pi_c})e_{ij}, & \pi < \pi_c \end{cases}$$

Here, $\pi = e_{ij}e_{ij}$ and e_{ij} is the (i,j)-th component of the deformation rate, π is the product of the component of the deformation rate with itself, π_c is a critical value of this product based on the non-Newtonian model, μ_B is the plastic dynamic viscosity of the non-Newtonian fluid, and p_y is the yield stress of the fluid.

The governing equations of such type of flow, in the usual notations, can be written as

$$\frac{\partial u}{\partial x} + \frac{\partial \upsilon}{\partial y} = 0 \tag{1}$$

$$u\frac{\partial u}{\partial x} + \upsilon\frac{\partial u}{\partial y} = u_e\frac{\partial u_e}{\partial x} + \nu\left(1 + \frac{1}{\beta}\right)\frac{\partial^2 u}{\partial y^2} \tag{2}$$

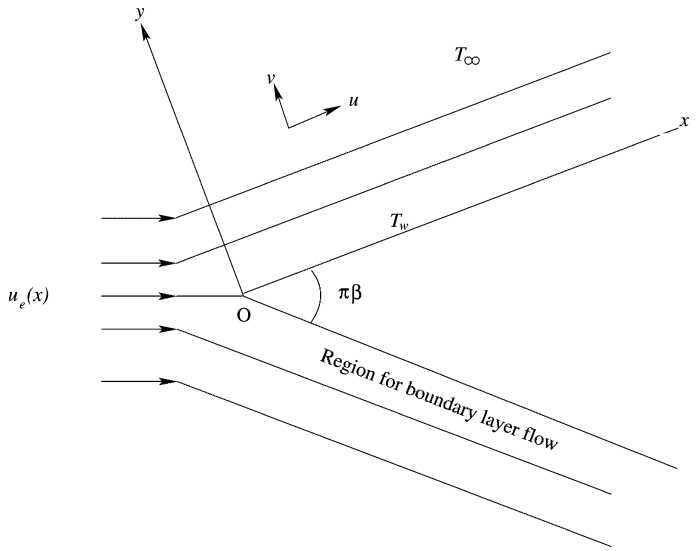

Fig. 1. Sketch of the physical problem and the coordinate system.

$$u\frac{\partial T}{\partial x}+\upsilon\frac{\partial T}{\partial y}=\kappa\frac{\partial^2 T}{\partial y^2} \tag{3}$$

where the viscous dissipation term in the energy equation is neglected due to its small value for an incompressible fluid motion. Here, u and v are the components of velocity in the x and y directions, respectively. While $\nu=\mu/\rho$ is the kinematic viscosity of the fluid, μ is the coefficient of fluid viscosity, ρ is the fluid density, β is the Casson parameter, T is the temperature, and κ is the coefficient of thermal diffusivity of the fluid.

2.1 Boundary conditions

The appropriate boundary conditions for the problem are given by

$$u=0,\upsilon=0,T=T_w \ \ at\ y=0 \tag{4}$$

$$u=u_e(x)=x^{\mathrm{m}},T\to T_\infty \ \ as \quad y\to\infty \tag{5}$$

where T_w is the wall temperature and T_∞ is the free stream or ambient temperature at infinity.

2.2 Method of solution

We now introduce the following relations for u, v as

$$u=\frac{\partial\psi}{\partial y},\upsilon=-\frac{\partial\psi}{\partial x} \tag{6}$$

where ψ is the stream function.

We also introduce the following dimensionless variables

$$\theta=\frac{T-T_\infty}{T_w-T_\infty} \tag{7}$$

$$\text{and}\ \ \eta=y\sqrt{\frac{\mathrm{m}+1}{2\nu}}\,x^{\frac{\mathrm{m}-1}{2}},\psi=\sqrt{\frac{2\nu}{\mathrm{m}+1}}\,x^{\frac{\mathrm{m}+1}{2}}f(\eta) \tag{8}$$

Using the relations (6) and (7) in the boundary layer Eq. (2) and in the energy Eq. (3), we get the following equations:

$$\frac{\partial\psi}{\partial y}\frac{\partial^2\psi}{\partial x\partial y}-\frac{\partial\psi}{\partial x}\frac{\partial^2\psi}{\partial y^2}=\mathrm{m}x^{2\mathrm{m}-1}+\nu(1+\frac{1}{\beta})\frac{\partial^3\psi}{\partial y^3} \tag{9}$$

$$\frac{\partial\psi}{\partial y}\frac{\partial\theta}{\partial x}-\frac{\partial\psi}{\partial x}\frac{\partial\theta}{\partial y}=\kappa\frac{\partial^2\theta}{\partial y^2} \tag{10}$$

The boundary conditions Eqs. (4) and (5) then become

$$\frac{\partial\psi}{\partial y}=0,\frac{\partial\psi}{\partial x}=0,\theta=1 \ \ at\ \ y=0 \tag{11}$$

$$\frac{\partial \psi}{\partial y} = x^{\mathrm{m}}, \theta \to 0 \ \ as \ \ y \to \infty \tag{12}$$

Using Eqs. (8), Eqs. (9) and (10) can finally be put in the following form:

$$\left(1+\frac{1}{\beta}\right) f''' + ff'' + \frac{2\mathrm{m}}{\mathrm{m}+1}(1-f'^2) = 0 \tag{13}$$

$$\frac{1}{\mathrm{Pr}}\theta'' + f\theta' = 0 \tag{14}$$

where $Pr = \nu/\kappa$ and the boundary conditions finally become

$$f'(\eta) = 0, f(\eta) = 0, \theta = 1, at \ \ \eta = 0 \tag{15}$$

$$f'(\eta) = 1, \theta \to 0 \ \ as \ \ \eta \to \infty \tag{16}$$

Equations (13) and (14) along with the boundary conditions are solved by converting them to an initial value problem. We set

$$f' = z, z' = p, p' = \left\{\frac{2\mathrm{m}}{\mathrm{m}+1}\left(z^2-1\right) - fp\right\} \Big/ \left(1+\frac{1}{\beta}\right) \tag{17}$$

$$\theta' = q, q' = -\mathrm{Pr}\, fq \tag{18}$$

with the boundary conditions

$$f(0) = 0, f'(0) = 0, \theta(0) = 1 \tag{19}$$

In order to integrate Eqs. (17) and (18) as an initial value problem, we require a value for $p(0)$ that is $f''(0)$ and $q(0)$ that is $\theta'(0)$ but no such values are given in the boundary conditions. The suitable guess values for $f''(0)$ and $\theta'(0)$ are chosen and then integration is carried out. We compare the calculated values for f' and θ at $\eta = 8$ (say) with the given boundary condition $f'(8) = 1$ and $\theta(8) = 0$ and adjust the estimated values, $f''(0)$ and $\theta'(0)$, to give a better approximation for the solution. We take the series of values for $f''(0)$ and $\theta'(0)$, and apply the fourth-order classical Runge–Kutta method with step-size $h = 0.01$. The above procedure is repeated until we get the converged results within a tolerance limit of 10^{-5}.

Table 1. Comparison of Values of $f''(0)$ for Variable Values of m for Newtonian Fluid

m	Yih [7]	Chamkha et al. [9]	Pal and Mondal [12]	Cebeci and Bradshaw [35]	Present study
-0.05	0.213484	0.213802	0.213484	0.21351	0.213802
0	0.332057	0.332206	0.332206	0.33206	0.332206
0.33	0.757448	0.757586	0.757586	0.75745	0.757586
1	1.232588	1.232710	1.232710	1.023259	1.232710

Table 2. Comparison of Values of $\theta'(0)$ for Variable Values of Prandtl number Pr with $m = 0$ for Newtonian Fluid

Pr	Lin and Lin [4]	Yih [7]	Chamkha et al. [9]	Pal and Mondal [12]	Present study
0.001	0.017316	0.017316	0.017381	0.017316	0.017316
0.01	0.051590	0.051589	0.051830	0.051589	0.051589
0.1	0.140032	0.140034	0.142003	0.140034	0.140034
1	0.332057	0.332057	0.332173	0.332057	0.332057
10	0.728148	0.728141	0.728310	0.728141	0.728141

For the verification of the accuracy of the applied numerical scheme, results for $f''(0)$ for various values of m and also for $\theta'(0)$ and different values of the Prandtl number Pr (with $m = 0$) in case of a Newtonian fluid are compared with those reported by Lin and Lin [4], Yih [7], Chamkha et al. [9], Pal and Mondal [12], and Cebeci and Bradshaw [35]. The results are found to be in excellent agreement which builds confidence that the present numerical results are accurate and the numerical method used is accurate. The comparisons are shown in Tables 1 and 2.

3. Results and Discussion

In order to analyze the results, numerical computation has been carried out for various values of the Falkner–Skan exponent m, Casson fluid parameter β, and the Prandtl number Pr. For illustrations of the results, numerical values are plotted in Fig. 2(a) through Fig. 5(c).

Figures 2(a) and 2(b) depict the effects of the Falkner–Skan exponent m on the velocity and temperature profiles, respectively. Figure 2(a) presents the effects of increasing m on the fluid velocity. With increasing values of the exponent m, the fluid velocity is found to increase. It is observed that in the case of an accelerated flow ($m > 0$), the velocity profiles have no point of inflection whereas in the case of decelerated flow ($m < 0$), they exhibit a point of inflection. Flow separation occurs at $m = -0.091$. For accelerated flows (i.e., positive values of m), the velocity profiles merely squeeze closer and closer to the wall, and backflow phenomena are not noted. Here, $m = 0$ presents the result for a flat plate. It is noted that the boundary layer thickness decreases as m increases, hence it gives rise to the velocity gradient, which in turn causes an increase in the skin friction [Fig. 2(a)]. Figure 2(b) exhibits that the temperature $\theta(\eta)$ in the boundary layer region decreases with increasing values of m. Since the thermal boundary layer thickness increases with m, it causes a decrease in the rate of heat transfer [Fig. 2(b)].

The effects of the Casson fluid parameter β on the velocity and temperature profiles are exhibited in Figs. 3(a) and 3(b), respectively. In this study we have considered the values of the Casson parameter in the range $0.2 \le \beta \le 5$. With increasing values of β, the fluid velocity increases but the temperature decreases in this case. Figure 3(a) clearly indicates that the thickness of the velocity boundary layer decreases. No point of inflection is observed for higher values of β [see Fig. 3(a)]. From this figure, it is very clear that flow separation can be controlled in the case of a non-Newtonian Casson fluid by increasing the value of the Casson fluid parameter. Figure 3(b) shows that the temperature decreases with increasing values of β. That is, the rate of heat transfer (the thermal

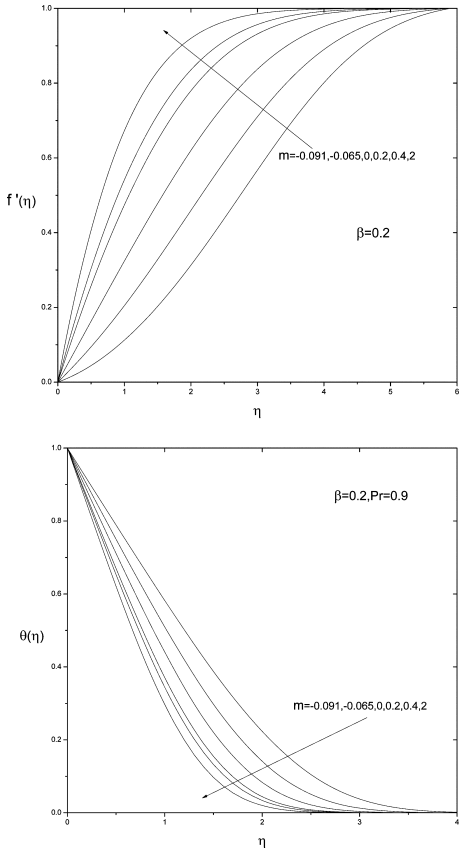

Fig. 2. (a) Velocity profiles for variable values of *m*; (b) temperature profiles for variable values of *m*.

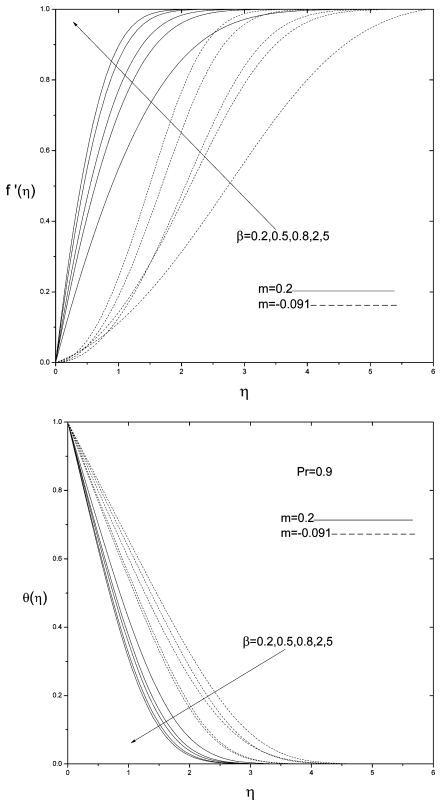

Fig. 3. (a) Velocity profiles for variable values of Casson parameter β; (b) temperature profiles for variable values of Casson parameter β.

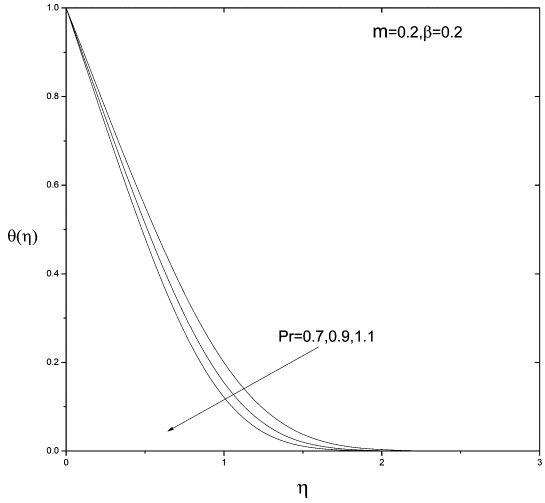

Fig. 4. Temperature profiles for variable values of Prandtl number Pr.

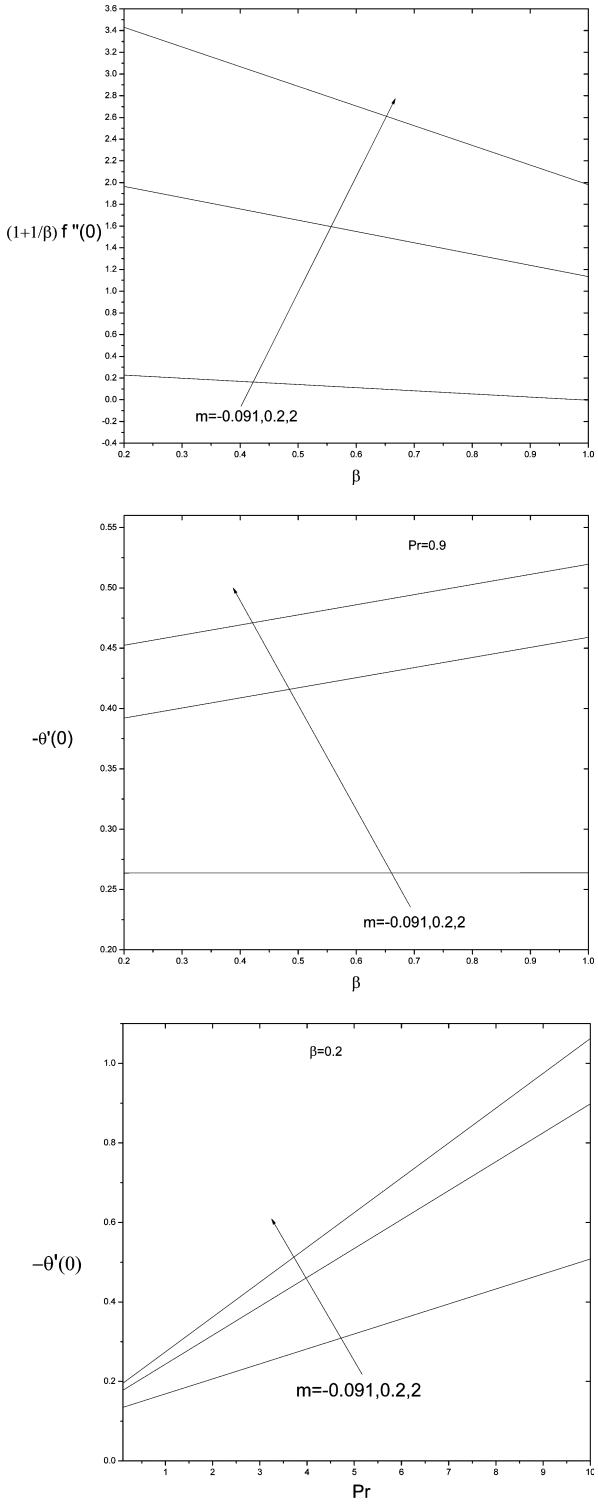

Fig. 5. (a) Variations of skin friction coefficient with Casson parameter β for various values *m*; (b) variations of heat transfer coefficient with Casson parameter β for various values of *m*; (c) variations of heat transfer coefficient with Prandtl number Pr for various values of *m*.

boundary-layer thickness becomes thinner) is enhanced when the velocity boundary-layer thickness decreases.

Figure 4 presents the effect of the Prandtl number on the temperature profile. With increasing values of the Prandtl number Pr, the temperature is found to decrease. This is in agreement with the physical fact that the thermal boundary-layer thickness decreases with increasing values of Pr.

Figure 5(a) exhibits the nature of the skin friction coefficient. It is very clear that the force due to the skin friction increases as the included angle of the wedge (β_1) increases, i.e., the skin friction coefficient increases with Falkner–Skan exponent *m* but it decreases with the Casson fluid parameter β. On the other hand, the heat transfer coefficient is found to increase with increasing values of *m*, β [Fig. 5(b)] and also with Pr [Fig. 5(c)]. It is noted that the values of $[-\theta'(0)]$ are always positive, i.e., the heat is transferred from the heated surface to the cold fluid (see, Yacob et al. [22]).

4. Conclusions

A numerical solution for the flow of a Casson fluid and heat transfer over a symmetric wedge is presented. A transformed set of self-similar equations is obtained and solved numerically by the Runge–Kutta method with the help of the shooting technique. With an increase in the Casson fluid parameter, the fluid velocity is found to increase whereas the temperature decreases. The non-dimensional temperature decreases with increasing values of the Prandtl number. A significant result obtained is that by increasing the values of the Casson fluid parameter, flow separation can be prevented. The rate of heat transfer increases with increasing values of the Falkner-Skan exponent, Casson fluid parameter, and the Prandtl number.

Acknowledgment

This work is supported by UGC, New Delhi, India under the Special Assistance Programme DSA Phase-1. Thanks are indeed due to the reviewers for the constructive suggestions which helped a lot in improving the quality of the article.

Literature Cited

1. Falkner VM, Skan SW. Some approximate solutions of the boundary-layer for flow past a stretching boundary. SIAM J Appl Math 1931;49:1350–1358.
2. Hartree DR. On equations occurring in Falkner and Skan's approximate treatment of the equations of boundary layer. Proc Cambridge Phil Soc 1937;33:223–239.
3. Hady FM, Hassanien IA. Effect of transverse magnetic field and porosity on the Falkner–Skan flows of a non-Newtonian fluid. Astrophys Space Sci 1985;112:381–390.
4. Lin HT, Lin LK. Similarity solutions for laminar forced convection heat transfer from wedges to fluids of any Prandtl number. Int J Heat Mass Transf 1987;30:1111–1118.
5. Watanabe T, Pop I. Magnetohydrodynamic free convection flow over a wedge in the presence of a transverse magnetic field. Int Commun Heat Mass Transf 1993;20:871–881.
6. Kafoussias NG, Nanousis ND. Magnetohydrodynamic laminar boundary-layer flow over a wedge with suction or injection. Can J Phys 1997;75:733–745.
7. Yih KA. Forced convection flow adjacent to a non-isothermal wedge. Int Commun Heat Mass Transf 1996;26:819–827.

8. Hossain MA, Munir MS, Rees DAS. Flow of viscous incompressible fluid with temperature dependent viscosity and thermal conductivity past a permeable wedge with uniform surface heat flux. Int J Therm Sci 2000;39:635–644.
9. Chamkha AJ, Quadri MM, Camille I. Thermal radiation effects on MHD forced convection flow adjacent to a non-isothermal wedge in the presence of a heat source or sink. Heat Mass Transf 2003;39:305–312.
10. Pantokratoras A. The Falkner-Skan flow with constant wall temperature and variable viscosity. Int J Therm Sci 2006;45(4):378–389.
11. Mukhopadhyay S. Effects of radiation and variable fluid viscosity on flow and heat transfer along a symmetric wedge. J Appl Fluid Mech 2009;2(2):29–34.
12. Pal D, Mondal H. Influence of temperature-dependent viscosity and thermal radiation on MHD forced convection over a nonisothermal wedge. Appl Math Comput 2009;212:194–208.
13. Kandasamy R, Periasamy K, Sivagnana Prabhu KK. Effects of chemical reaction, heat and mass transfer along a wedge with heat source and concentration in the presence of suction or injection. Int J Heat Mass Transf 2005;48:1388–1394.
14. Hossain MA, Bhowmik S, Gorla RSR. Unsteady mixed-convection boundary layer flow along a symmetric wedge with variable surface temperature. Int J Eng Sci 2006;44:607–620.
15. Kim YJ. Thermal boundary layer flow of a micropolar fluid past a wedge with constant wall temperature. Acta Mech 1999;138:113–121.
16. Kim YJ, Kim TA. Convective micropolar boundary layer flows over a wedge with constant surface heat flux. Int J Appl Mech Eng 2003;8:147–153. [Special issue: ICER 2003]
17. Ishak A, Nazar R, Pop I. MHD boundary-layer flow of a micropolar fluid past a wedge with constant wall heat flux. Commun Nonlinear Sci Numer Simul 2009;14:109–118.
18. Riley N, Weidman PD. Multiple solutions of the Falkner-Skan equation with suction or injection. J Appl Math Comput 1989;25:67–83.
19. Ishak A, Nazar R, Pop I. Moving wedge and flat plate in a micropolar fluid. Int J Eng Sci 2006;44:1225–1236.
20. Ishak A, Nazar R, Pop I. Falkner Skan equation for flow past a moving wedge with suction or injection. J Appl Math Comput 2007;25:67–83.
21. Kandasamy R, Muhaimin, Hashim I, Ruhaila. Thermophoresis and chemical reaction effects on non-Darcy mixed convective heat and mass transfer past a porous wedge with variable viscosity in the presence of suction or injection. Nuclear Eng Design 2008;238:2699–2705.
22. Yacob NA, Ishak A, Pop I. Falkner-Skan problem for a static or moving wedge in nanofluids. Int J Therm Sci 2011;50:133–139.
23. Mukhopadhyay S. Upper-convected Maxwell fluid flow over an unsteady stretching surface embedded in porous medium subjected to suction/blowing. Z Naturforsch 2012;67a:641–646. DOI: 10.5560/ZNA.2012-0075
24. Mukhopadhyay S, Vajravelu K. Effects of transpiration and internal heat generation/absorption on the unsteady flow of a Maxwell fluid at a stretching surface. ASME J Appl Mech 2012;79:044508-1.
25. Patel V, Timol MG. Similarity solutions of the three dimensional boundary layer equations of a class of general non-Newtonian fluids. Int J Appl Math Mech 2012;8:77–88.
26. Mustafa M, Hayat T, Pop I, Aziz A. Unsteady boundary layer flow of a Casson fluid due to an impulsively started moving flat plate. Heat Transfer-Asian Res 2011;40(6):563–576.
27. Mustafa M, Hayat T, Pop I, Hendi A. Stagnation-point flow and heat transfer of a Casson fluid towards a stretching sheet. Zeitschrift für Naturforschung A 2012;67a(1/2):70–76.
28. Bhattacharyya K, Hayat T, Alsaedi A. Analytic solution for magnetohydrodynamic boundary layer flow of Casson fluid over a stretching/shrinking sheet with wall mass transfer. Chin Phys B 2013;22(2):024702.

29. Singh S. Clinical significance of aspirin on blood flow through stenotic blood vessels. J Biomimetics, Biomaterials, and Tissue Eng 2011;1314(10):17–24.
30. Nadeem S, Ul Haq R, Lee C. MHD flow of a Casson fluid over an exponentially shrinking sheet. Scientia Iranica 2012;19(6):1550–1553.
31. Kandasamy A, Pai RG. Entrance region flow of Casson fluid in a circular tube. Appl Mech Mater 2012;110-116:698–706.
32. Eldabe NTM, Salwa MGE. Heat transfer of MHD non-Newtonian Casson fluid flow between two rotating cylinders. J Phys Soc Jpn 1995;64:41–64.
33. Dash RK, Mehta KN, Jayaraman G. Casson fluid flow in a pipe filled with a homogeneous porous medium. Int J Eng Sci 1996;34(10):1145–1156.
34. Nakamura M, Sawada T. Numerical study on the flow of a non-Newtonian fluid through an axisymmetric stenosis. J Biomech Eng 1988;110(2):137–143.
35. Cebeci T, Bradshaw P. Physical and computational aspects of convective heat transfer, 1st ed. Springer-Verlag; 1984.

□♦ ♦ ♦□